



Investigation of Solar Chimney Power Plant and Experimental Analysis of Energy Yield from Small Size Draft Tube and Solar Collector

Ashenafi Tesfaye Bicks^{1(✉)}, Solomon Tesfamariam Teferi²,
and Tewodros Walle Mekonnen²

¹ Department of Mechanical Engineering, University of Gondar,
Gondar, Ethiopia

² Addis Ababa Institute of Technology, Addis Ababa University,
Addis Ababa, Ethiopia

Abstract. The Solar chimney power plant is a naturally driven power generating system. In this research, a solar chimney power plant is studied by developing an experimental model for a maximum power output of 32 W. The performance of large-scale electricity generation from the plant is predicted by analyzing different geometrical configurations. CFD model is used to study flow characteristics of air temperature inside the collector. Then, for 30 kW power output, the selected optimized dimensions are: chimney height, collector diameter, chimney diameter, and collector height are estimated to be 15 m, 15 m, 0.2 m, and 0.2 m respectively. For a fixed chimney diameter and collector height, an increase in height of the chimney raises the power output until it reaches the designed optimum height, an increase in chimney height beyond the optimum value will result in an energy loss due to lower total pressure difference caused by frictional pressure rise. The experimental model developed is scaled down to a chimney height of 3 m and collector diameter of 2 m with a maximum power output of 32 W. In the experiment, the characteristics of the temperature inside the collector are studied by varying the height of the collector above the ground. The temperature difference between collector exit and collector inlet from the comparison of experimental and simulated modeled are in good agreement. It was found that the implementation of a solar chimney power plant is technically feasible for the generation of electrical energy up to the desired potential by adjusting chimney height and collector diameter.

Keywords: Solar energy · Solar chimney power plant · Solar collector · Optimum chimney height · Collector height

1 Background

The cause for the serious environmental problem is primarily an increase in global fossil fuel consumption for electrical energy generation and other needs. According to the study by different experts, it was predicted that if we do not shift the source of energy generation to a cleaner source, climate change will cause a significant problem

in our universe. Today, fossil fuels are the primary fuel source and are still widely used for major electricity generation around the world. According to the report of (Renewable and Agency 2017), the energy consumption for electricity production worldwide is projected to increase up to 2040 G.C.

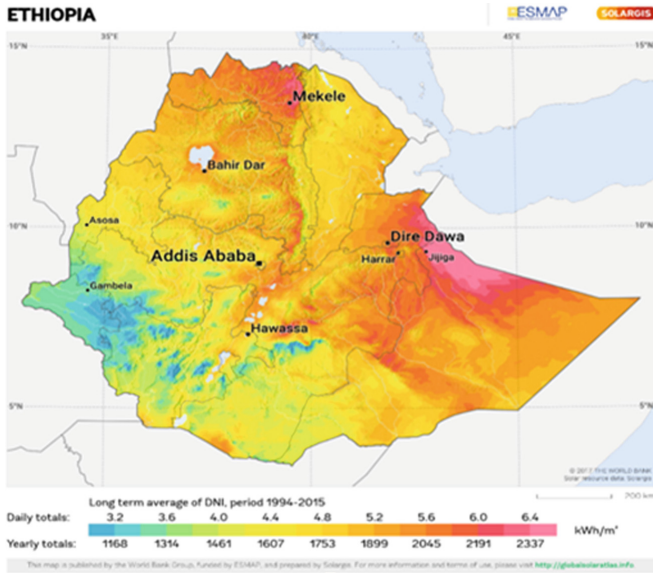


Fig. 1. Ethiopian Solar resource map (Renewable and Agency 2017)

Clean Electrical energy can be generated by a different mechanism using solar energy and other natural resources worldwide. For example, in developing countries like Ethiopia, it is estimated that a daily solar radiation potential varies between (3.2–6.4) kWh/m^2 as shown in Fig. 1. However, based on a report by (Renewable et al. 2012) electrical energy generation majority share (92.5%) comes from hydro-power, which only covers 38% of the total energy demand of the population. It can be concluded that the conversion of solar energy resources into useful energy is at its primary stage.

The solar chimney power plant is a form of solar energy conversion system, which is studied by several researchers in various countries but the first pilot plant of the solar chimney power plant was built in Spain in 1982. The project was functional for more than 8 years but it was considered inefficient as a result different researcher has conducted an experiment and made an improvement in its performance (Gannon and Backström 2003). The solar chimney power plant is a naturally driven power generating system. It converts solar energy first into thermal energy then into kinetic energy finally into electrical energy. It combines the concept of solar air collectors and a central updraft chimney to generate a solar-induced convective flow which drives turbines to generate electricity. Electricity generation from solar radiation by air convection works when the air beneath the collector gets heated, its density decreases. The buoyance force and the

pressure difference between the top and base of the chimney push the air upward. Part of this heat is converted to mechanical energy by the axial flow turbine mounted at the base of the chimney.

In 2010, (Koonsrisuk et al. 2010), Studied the effect of tower area change in a solar chimney power plant. The study showed that the tower area change affects the efficiency and the mass flow rate through the plant. The velocity increases at the top of a convergent tower, the mass flow rate remains similar to that of a constant area tower. For a divergent tower design, velocity increases near the base of the chimney, and the maximum kinetic energy also occurs at the base of the chimney.

In 2010 (Hamdan 2010), studied an analytical model. In the analysis, it is considered that a simplified Bernoulli's equation combined with fluid dynamics and ideal gas equation using EES solver to predict the performance of the solar chimney power plant. The study showed that the height and diameter of the solar chimney are the most important design variables for solar chimney power plants. However, the collector area has a small effect on second-law efficiency but a strong effect on harvested energy. (Ming et al. 2016), established a simple analysis of the air flowing through the solar chimney power plant and also studied the thermodynamic cycle of the solar chimney power plant. They also developed a mathematical model of ideal and actual cycle efficiencies for medium-sized and large-sized solar chimney power plants. Brayton cycle corresponding to medium-scale solar chimney power generation system is 1.33% and 0.3% respectively, while the ideal efficiency of large scale SC system with chimney height 1000 m is 3.33%, while the maximum value of the actual efficiencies is 0.9%. The results from their work were used as a theoretical guideline for designing and building a commercial-size solar chimney power plant in China.

In 2019 (Fallah and Valipour 2019), investigated the performance of solar chimney power plants with and without artificial roughness using a three-dimensional simulation. In the analysis, without artificial roughness, the airflow in the collector accelerates gradually and runs centripetally to the base of the chimney with energy being absorbed from the ground surface of the collector, and average velocity at the base of the chimney reaches 9.25 m/s. Also, the power of the SCPP is equal to 46.1 kW. But with artificial roughness, the negative influences are evident, creating friction in the flow path, the airflow at the chimney bottom is deflected with an average velocity of less than 9.25 m/s and it reaches 8.88 m/s and the power is reduced by about 5%. It is found that the artificial roughness in SCPP improves heat transfer, but reduces velocity; therefore, there is an optimal dimension and location for it. Geometrically, the location of this roughness near the collector entrance has a better performance than other locations, but this change of locations has little impact on the performance of SCPP.

In a solar chimney power plant system turbine is the main component which will be used as the power-producing unit. The main purpose of the turbine is to convert the kinetic energy of heated air into mechanical energy using the turbine rotors. To have easier installation and maintenance turbines are usually placed at the base of the chimney. The turbine of SCPP is usually an axial flow type turbine. The operation and design of modern wind turbines could be applied to the solar chimney but in comparison, solar chimney turbines have a much higher energy extraction per unit flow and are more similar to gas turbines. Solar chimney turbines have a greater pressure drop than wind turbines and require more blades but not as many as gas turbines. It was

found that wind turbine blades can be treated accurately as individual airfoils. This is not the case in the solar chimney turbine due to the higher blade solidity (blade chord to pitch ratio). The pitch angle of the blades can be adjusted like wind turbines but due to the flow being enclosed in an SSCP like a gas turbine, the turbine may have radial inflow guide vanes. The blades required for the solar chimney turbine are of low solidity when compared to gas-turbine turbo machinery but they cannot be treated accurately as single blades like those of wind turbines (von Backström and Gannon 2004).

Under this study, a small-scale solar chimney power plant is designed and experimentally investigated for the generation of 30 kW electrical energy. The optimum geometry for the desired output is analyzed by varying collector diameter, chimney height, and chimney diameter. The experimental model is designed to validate the simulation conducted using the CFD model. The developed model is scaled down to a chimney height of 3 m and collector diameter of 2 m for simplicity during an investigation. Using the CFD model the analyzed power output for a chimney height of 3 m, collector diameter of 2 m, 0.16 m chimney diameter, and 0.17 collector height from the ground provides 32 W power output which is 6% higher than the actual experiment of the same geometrical size. The measured data in the experimental result is 93.75% reliable with a deviation of 6.25% relative to the simulated result. The variation is mainly caused by the weather condition instability since the drought occurred in 2015 (USAID 2016). As a result recorded value between the CFD and experimental model is maximum since during the testing process the solar radiation intensity is not steady as anticipated in the historical data Moreover analysis is conducted for the prediction of maximum power output from this plant within the geometrical size of chimney height up to 60 m and collector diameter up to 25 m by fixed chimney diameter at 0.2 m and collector height at 0.2 m.

2 Material and Methods

a. Design of Solar Chimney Power Plant: A Case Study

The study of a solar chimney power plant is performed by combining, a theoretical design of technical parameters and simulation of the main component using CFD tools. To select a geometrical configuration for desired 30 kW power out, MATLAB software is used as an optimization tool. For the analysis of temperature and thermal characteristics inside the collector, ENERGY 2D is used as computational fluid dynamics (CFD) tool, it is also used to simulate the temperature variation in all dimensions of Collector sides. The actual prototype shown in Fig. 2 is designed to generate power out of 32 W maximum. The axial flow turbine is installed in between the collector exit and chimney inlet and the generator is placed at the ground beneath the turbine.



Fig. 2. Experimental Solar chimney power plant at the test site.

For the design of the solar chimney power plant, a mathematical equation is developed by considering the basic concept of conservation of energy, thermodynamic, momentum, and continuity equation. The collector material used in the experimental model is polyvinyl chloride (PVC) with optical property shown in Table 1.

Table 1. Optical property of polyvinyl chloride collector material

Material	Symbol	Value
Collector absorptivity (PVC)	α_c	0.3
Collector transmissivity	τ_c	0.7
Collector roughness length	e_{rc}	0.002 m
Emissivity of canopy	ξ	0.85

i. Air standard cycle of SCPP cycle and the surrounding air expansion

In a solar chimney power plant (SCPP) cycle analysis compression takes place in the environment as shown in Fig. 3, this makes the cycle different from the gas turbine cycle where the compression takes place in the system. In an ideal gas turbine power, the expansion process entirely takes place inside the turbine. However, in solar chimney power plant expansion takes place first in the turbine in processes 2–3, and the remaining takes along the chimney system. Cooling process 4–5 is not inside the power plant. The exhaust air is mixed with the ambient air at state 5 and cooled back to state 1 as shown in Fig. 4.

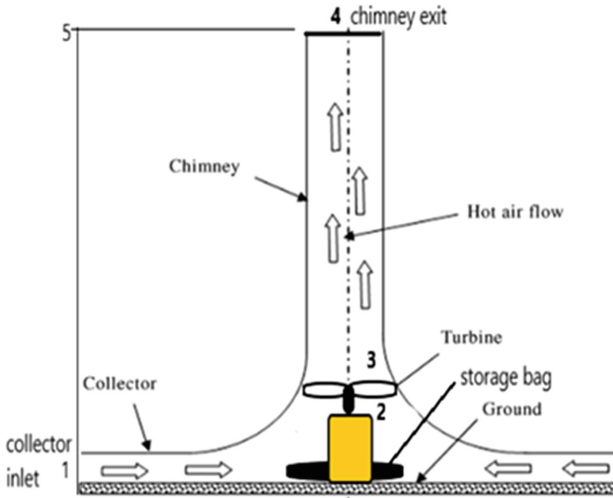


Fig. 3. Solar chimney power plant with generator and storage unit.

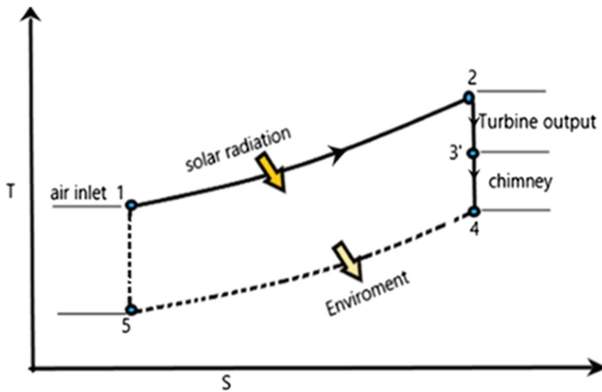


Fig. 4. T-S diagram of solar chimney power plant air standard cycle

The total heat input is;

$$Q_i = \dot{m} \times (h_2 - h_1) = \dot{m}C_p(T_2 - T_1) \tag{1}$$

The Expansion energy to lift the air to state 4:

$$P_{lift} = \dot{m} \times g \times H_{chim} \tag{2}$$

The energy exchange is isentropic since the friction and heat transfer are negligible. Then the value of enthalpy (Δh) can be equated to the amount of air that has descended in the atmosphere after having been cooled from chimney exit temperature. So, the enthalpy change in the chimney becomes;

$$\Delta h = g \times \Delta H_{chim} = Cp \times (T_1 - T_5) \tag{3}$$

Then the turbine shaft power becomes;

$$P_{shaft} = \dot{m} \times Cp \times (T_2 - T_3) - \dot{m} \times Cp \times (T_1 - T_5) \tag{4}$$

ii. **Momentum equation**

Figure 5 shows the instantaneous fluid flow through the area beneath the collector.

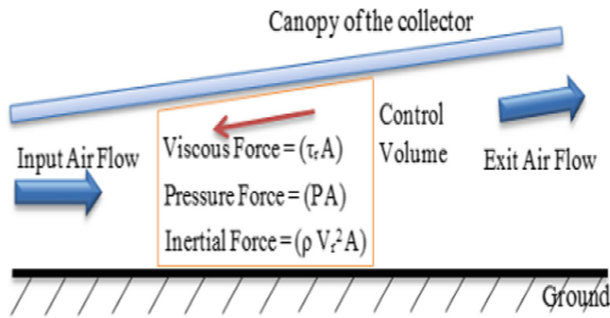


Fig. 5. The force that acts inside the bottom of the collector

Balance of forces of airflow inside the collector can be obtained by applying Newton’s second law for partial control volume:

$$\frac{\partial(\rho V_r^2)}{\partial r} = -\frac{\partial P}{\partial r} + \frac{\partial \tau_r}{\partial r} + \rho g \tag{5}$$

iii. **Continuity equation**

The continuity equation of the collector for radial flow shown in Fig. 6 is written as;

$$(\rho_1 V_r A_{COLL})_{in} = (\rho_2 V_r A_{COLL})_{out} \tag{6}$$

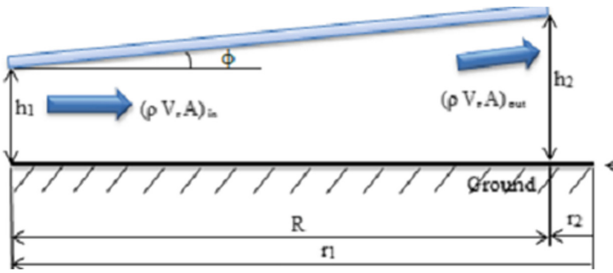


Fig. 6. Radial section of the collector

iv. Energy Conservation

The total energy per area of the collector shown in Fig. 7 is the sum of;
 Heat gain into the glazing = heat lost from the glazing
 Heat gain into the absorber = heat lost from the absorber
 Heat gain into the fluid = heat lost from the fluid
 Heat gain into the ground = heat lost from the ground

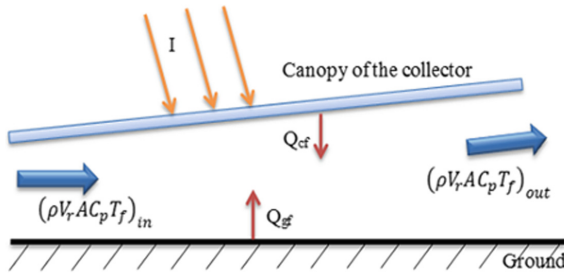


Fig. 7. Energy balance diagram for SCPP system.

In a solar chimney power plant, the flow of the fluid is due to natural convection. Natural convection is when the fluid is driven by local density difference while mixed convection flows occur when the convection of fluid is driven by both a pressure gradient and buoyancy forces. The resistance diagram for all heat transfer modes in the solar chimney power plant system is shown in Fig. 8.

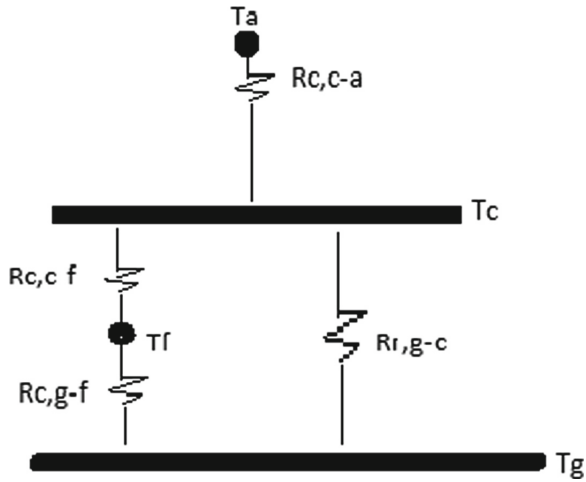


Fig. 8. Resistance diagram for all heat transfer modes in SCPP

In the CFD analysis, the model is investigated by the characteristics of the fluid flow inside the collector shown in Fig. 9. In the simulations, steady-state analysis is considered by creating an environment of updraft solar chimney power plant as per the design.

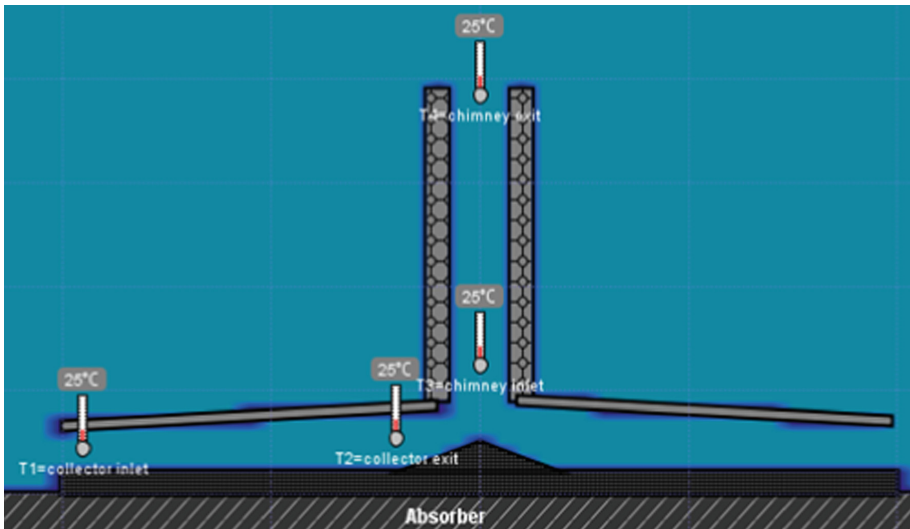


Fig. 9. Thermal boundary condition setting

b. Design methodology

To calculate the available power output from the plant an assumption for pressure ratio between chimney inlet, (P3) and collector exit (P2) will be made initially as, P_3/P_2 . The collector inlet pressure P1 is assumed as $P_{atm} = 0.77$ bar (atmospheric pressure at inlet @ $T_1 = 25^\circ\text{C}$). This power plant is open to the environment, pressure variation between the collector inlet and collector exit is neglected. By considering the number stationed in Fig. 3 all the parameters are equated as follows.

The collector exit temperature is found from the energy equation;

$$q''A_{gz} = \frac{1}{2}\dot{m} \times (v_2^2 - v_1^2) + \dot{m} \times Cp(T_2 - T_1) \quad (7)$$

According to (Koonsrisuk and Chitsomboon 2013) frictional effect is ignored since the velocity in this region is quite low. Because the flow is in the very low Mach number regime, the kinetic energy contribution can be neglected.

Then the above equation will be re-written as:

$$q''A_{gz} = \dot{m}Cp(T_2 - T_1) \quad (8)$$

This shows that the mass flow rate is inversely proportional to the collector temperature rise, Since the mass flow rate is assumed to be constant, then collector area can be found from (Koonsrisuk and Chitsomboon 2013) equation.

$$T_2 = T_1 + \frac{q''A_{gz}}{\dot{m}Cp} \quad (9)$$

Heat flux q'' incident on the surface of the glazing, with an overall heat loss coefficient value of: $U_t = 5 \text{ W/m}^2\text{K}$

$$q'' = (\alpha \times \tau) \times G_r - U_t \times \Delta T \quad (10)$$

The work extraction process at the turbine is assumed to be an isentropic process, Temperature of air at the entrance of chimney or turbine exit (T_3) can be calculated from the equation below;

$$T_3 = T_2 \left(P_3/P_2 \right)^{\frac{\gamma-1}{\gamma}} \quad (11)$$

Then the pressure P_4 at the chimney exit can be found from the following equation;

$$P_4 = P_1 \left(1 - \left(\frac{g^* H_{chim}}{Cp^* T_1} \right)_{Cp/R} \right) \quad (12)$$

From the ideal gas constant the density of each state can be written as;

$$\rho = \frac{P}{RT} \quad (13)$$

To determine the density at the chimney outlet the temperature at that state should be known; According to the (Backström et al. 2000) equation of temperature at chimney exit T_4 becomes;

$$T_4 = T_3 - g \times \frac{H_{chim}}{C_p} \quad (14)$$

Now recall that the above parameter is computed by the assumed value of pressure P_3 , so this result has to be validated by equation developed by (Backström et al.2000) for actual P_3 .

Pressure at the chimney inlet or turbine outlet;

$$P_{3actual} = P_4 + 0.5 \times (\rho_3 + \rho_4) \times g \times H_{chim} + \left(\frac{\dot{m}}{A_{gz}} \right) \left(\frac{1}{\rho_4} - \frac{1}{\rho_3} \right) \quad (15)$$

The tower (chimney) converts the heat flow produced by the collector into kinetic energy (convection current) and potential energy (pressure drop at the turbine). The density difference caused by the temperature rise in the collector works as a driving force.

The lighter column of air in the tower is connected with the surrounding atmosphere at the base (inside the collector) and the top of the tower, and thus acquires lift. The pressure difference Δp_{tot} is produced between tower base (collector outlet) and the ambient;

The pressure difference can be written as;

$$\Delta p_{tot} = g \times \int_0^{H_{chim}} (\rho_2 - \rho_4) dH \quad (16)$$

The pressure difference can be re-written as;

$$\Delta p_{tot} = g \times (\rho_2 - \rho_4) \times H_{chim} \quad (17)$$

The useful driving pressure is;

$$P_t = \Delta p_{tot} - P_f \quad (18)$$

Where P_f = frictional pressure drops.

Then the velocity at the chimney entrance V_2 can be found from (Zhou et al. 2010);

$$V_2 = \frac{G(\tau \times \alpha) \times A_{gz} - \beta(\Delta T_a \times A_{gz})}{\rho_{air} A_{chim} c_p (\Delta T)} \tag{19}$$

Then, $\Delta T_a = (T_{pm} - T_1)$.

i. Mean plate temperature (T_{pm})

$$T_{pm} = T_1 - \frac{Q_{useful}}{A_{gz} \times \beta \times F_R} \times (1 - F_R) \tag{20}$$

ii. Collector Heat removal factor (F_R)

$$F_R = \frac{\dot{m} \times C_P}{A_{gz} \times \beta} \left(1 - \exp\left(\frac{A_{gz} \times \beta \times F'}{\dot{m} \times C_P} \right) \right) \tag{21}$$

The theoretical **power extracted** by the turbine can be determined from the energy equation and Gibbs relation from classical thermodynamics;

$$P_{out} = \eta_{tur} \times P_t \times V_2 \times A_{gz} \tag{22}$$

So, to calculate the theoretical power output using Eq. (22), the solution procedure is shown in Fig. 10 has to be followed. The power output from this plant is mainly dependant on the area of the collector, chimney diameter, and chimney height so it can be seen that increasing the area of the collector will have a direct impact on power output, so the longer the collector diameter the higher the power output, the total pressure P_t is also the effect of chimney height and diameter so an increase in two parameters will result in increased power output. The atmospheric pressure is assumed to be below 1 bar at the collector exit or chimney inlet (P_2) due to the shape of a low-pressure trough (dome). The pressure is lower at this point due to warm air advection. At the collector exit and chimney inlet, the warm air is less dense than the air replacing it, as a result, surface pressure at P_2 will fall below 1 bar. The pressure at collector inlet pressure P_1 is assumed to be the same as the pressure in the collector exit for simplicity during analysis.

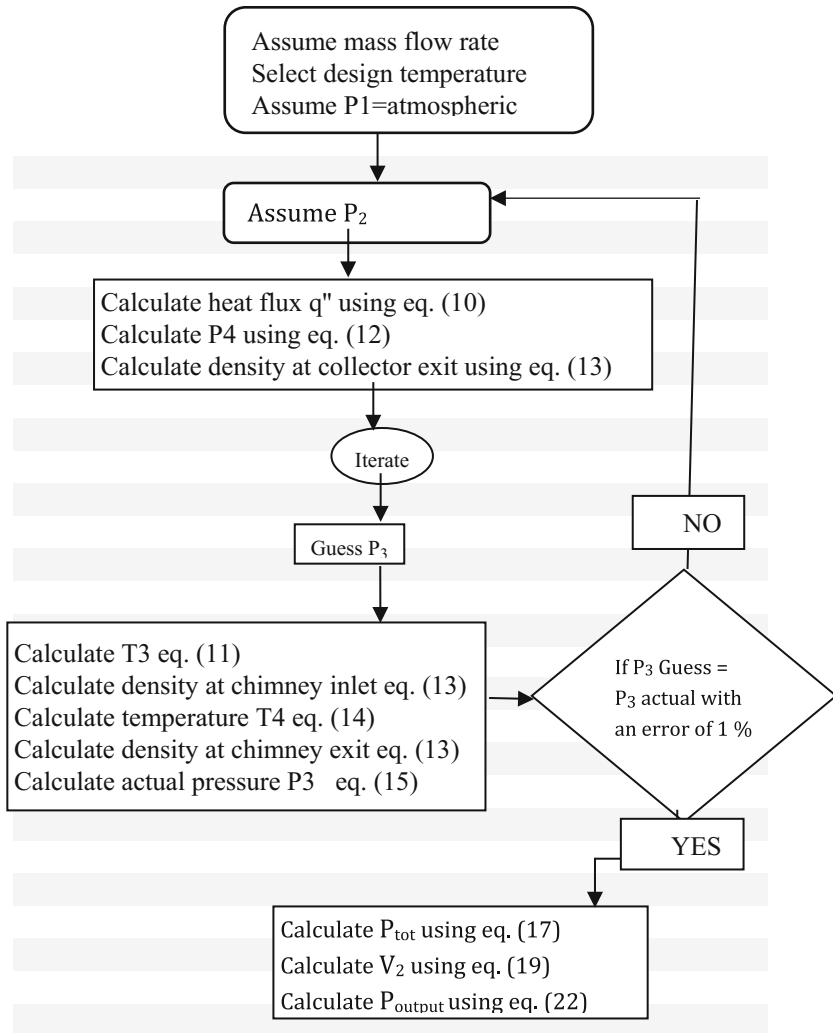


Fig. 10. Solar chimney power output solution procedure

3 Result and Discussion

In this study, the optimum geometrical size of the solar chimney power plant main component is selected at different collector diameter, chimney height that provides maximum power output. In the analysis, the influence of different parameters on the power output has been investigated as shown in the following sections.

3.1 Optimization of Solar Chimney Power Plant for Different Geometrical Size

I. Power Output vs Diameter of Glazing (Collector)

In the analysis, the variation of power output with an increase in a collector diameter is simulated by fixing the diameter of a chimney at 200 mm, the height of the collector from the ground at 200 mm, and varying the height of the chimney from 5 m–15 m as shown. According to the result shown in Fig. 11, the power output increases linearly with an increase in collector diameter and chimney height. In the investigation, it was seen that an increase in diameter of the collector creates a good condition to an inlet air to gain more heat until it reaches to chimney inlet since the longer air it takes the air to reach the collector exit the more it gets heated.

The analysis conducted was used to predict the optimum geometrical size for the 30 kW power output. As a result chimney height of 9 m and collector diameter of 22 m is optimum size as shown in Table 2. It should be noted that collector diameter should be as minimum as possible to reduce the area coverage by the plant. Additionally, the analysis showed that using the indicated fixed-parameter a chimney height must be more than 6 m to reach the desired power output. This can be varied by (Dehghani and Mohammadi 2014); they presented an optimal geometrical selection based on need and population size. In the analysis, the simulated Scatter distribution of the collector diameter with population, accordingly for a population size of the optimal range of collector diameter is between 200 and 1200 m while the allowable range is between 100 and 1500 m at an indicated other fixed geometrical area and total cost.

Table 2. Geometry selection for 30kW for power output

Options	Geometry				Power(kW)
	<i>Hchim</i>	<i>hc1</i>	<i>Dcoll</i>	<i>Dchim</i>	
1	3 m	200 mm	30 m	200 mm	15 kW
2	6 m	200 mm	28 m	200 mm	30 kW
3	9 m	200 mm	22 m	200 mm	30 kW
4	12 m	200 mm	16 m	200 mm	30 kW
5	15 m	200 mm	13 m	200 mm	30 kW

II. Height of Chimney Versus Power Output

The result shown in Fig. 12 was conducted by varying the height of the chimney and diameter of the collector while fixing the diameter of the chimney and collector height from the ground at 200 mm each. The result shown in Fig. 12 illustrates the optimum chimney height that gives the maximum power output for a certain collector diameter, chimney height, and collector height from the ground. For the case study under consideration, for simplicity and less collector area coverage, option three (3) is selected for the application of 30 kW power output, with a chimney height of 17 m and 17 m of collector diameter as shown in Table 4. Moreover, by keeping the fixed parameters and

increasing the chimney height up to 45 m and the collector diameter of 25m more than 350 kW power output can be achieved as shown in Fig. 11. However, increasing the chimney height above 45 m will result in power loss caused by the total frictional pressure drop in the chimney (draft tube) system.

It can be verified based on the investigation carried out by (Asnaghi and Ladjevardi 2012); they conducted an investigation in energy generation from the solar chimney power plant at 4 selected regions in Iran. According to their analysis, the considered solar chimney power plant is predicted to produce electrical power from 175 MWh–265 MWh in different months of the year. In the analysis, it is assumed that the turbine can create a 120 Pa pressure difference with an overall conversion efficiency of 4%.

Table 3. Chimney height selection for 30 kW

Options	Geometry				Power (kW)
	<i>Dchim</i>	<i>Dcoll</i>	<i>Hchim</i>	<i>hc1</i>	
1	200 mm	5 m	60 m	200 mm	21 kW
2	200 mm	10 m	28 m	200 mm	30 kW
3	200 mm	17 m	17 m	200 mm	30 kW
4	200 mm	20 m	9 m	200 mm	30 kW
5	200 mm	25 m	7 m	200 mm	30 kW

3.2 CFD Analysis of Solar Chimney Power Plant with Same Geometrical Size to the Experiment

a) Height of Chimney vs Power Output

For specific geometrical setup listed in Table 3, an increase in the height of the chimney above 62 m at fixed collector height from the ground ($hc_1 = 170$ mm), the diameter of the chimney ($D_{chim} = 160$ mm), the diameter of the collector ($D_{coll} = 2$ m) will result in a decrease in power output generation, the decrease in the power is caused by the domination of a frictional pressure along with the chimney(draft tube). When a chimney height reaches 107 m the power output equal to zero means frictional pressure loss is equal to useful driving pressure. Therefore, for the indicated fixed parameters shown the optimum chimney height for useful energy production is 58 m as shown in Fig. 13.

Table 4: Geometry specification for a model developed

No.	Parameter	Value	Symbol
1	Chimney height	3 m	H_{chim}
2	Collector diameter	2 m	D_{coll}
3	Chimney diameter	0.16 m	D_{chim}
4	Collector height from the ground	0.170–0.4 m	hc_1

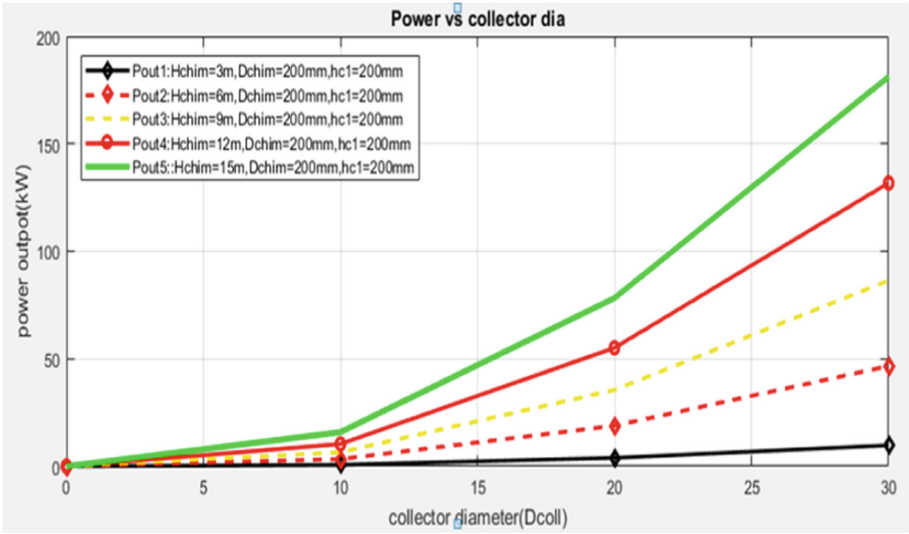


Fig. 11. collector diameter vs power output.

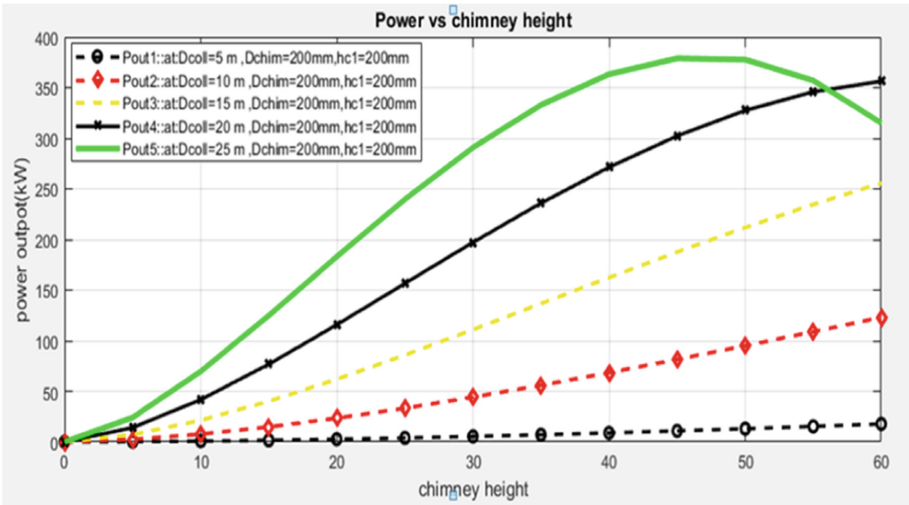


Fig. 12. Chimney height versus power output



Fig. 13. Power versus chimney height for experiment

The experimental study under consideration, the developed model of the solar chimney power plant is constructed with 3-m chimney height and 2-m collector diameter (with an aperture area of 3.97 m^2) which provides a maximum power output of 32 W as shown in Fig. 13. Under a fixed chimney height from the ground ($hc1 = 0.170 \text{ m}$), collector diameter ($D_{\text{coll}} = 2 \text{ m}$), and chimney diameter ($D_{\text{chim}} = 0.16 \text{ m}$), the optimum chimney height is 52 m, an increase in chimney height beyond 52 m will result in power loss due to frictional pressure drop in a chimney.

b) Collector Diameter vs. Power Output

According to the analysis shown in Fig. 14, for a fixed chimney height from the ground ($hc1 = 0.170 \text{ m}$), collector diameter ($D_{\text{coll}} = 2 \text{ m}$) and chimney diameter ($D_{\text{chim}} = 0.16 \text{ m}$), an increase in the diameter of the collector up to 3 m will increase the power output of the plant up to maximum power output of 9 kW. When the collector diameter exceeds more than 5 m, the rate of power production increases more than twice. As a result, it can be concluded that solar chimney power plant is more economical for larger-scale than small-scale electrical power generation.

c) Pressure (P_t) Versus Height of the Chimney

At a fixed parameter of chimney diameter, collector diameter, collector exit temperature, and height of the collector from the ground of 0.16 mm, 2 m, 315 K and 0.17 mm respectively. The useful pressure (P_t) increases until the chimney height reaches 58 m, beyond this height of the chimney the pressure tends to dramatically drop down due to

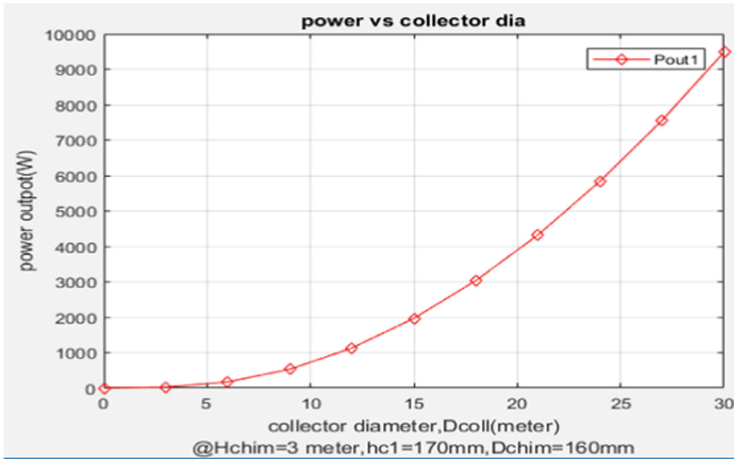


Fig. 14. Power output versus collector diameter idea that solar

the cumulative effect of frictional pressure loss. At a fixed parameter useful pressure is zero when the chimney height reaches 103 m this results in zero power output of the solar chimney power plant. So, the maximum allowable chimney height for this designed solar chimney power plant is 58-m unless if the is no change in the fixed-parameter as shown in Fig. 15.

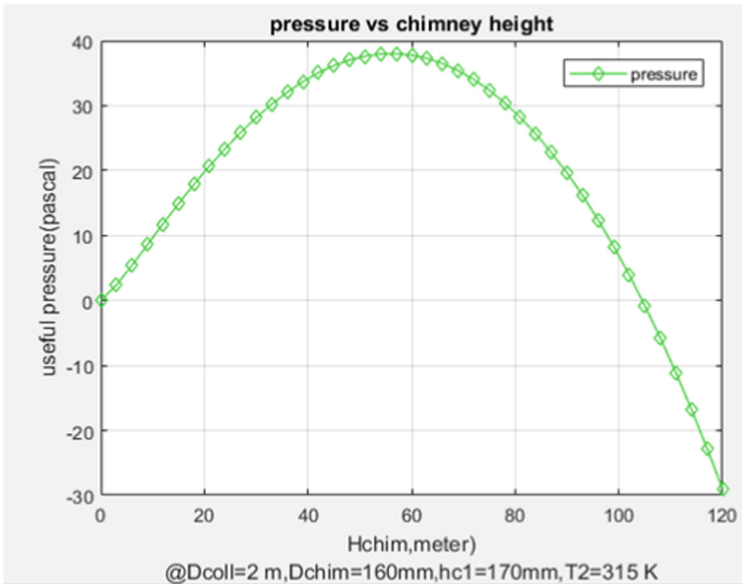


Fig. 15. Useful Pressure versus chimney height

3.3 Actual Prototype Experimental Result

In the experimental analysis the temperature is recorded for three consecutive days starting from May 21/18–May 23/18 for collector height of the 170 mm and 400 mm from the ground as shown in Fig. 16. An average was taken in every 5-min recording due to the instability of the weather condition. The maximum collector exit temperature reading of 41.7 °C was recorded at mid-day at 12 : 44 h. This can be validated by the experimental investigation conducted by (Lal et al. 2016), according to their study the maximum air temperature and velocity in the collector area are found to be 42.4 °C and 12.2 m/s respectively at 14:00 h of the typical day with approximately with the same geometrical size compared to prototype in this study. The maximum solar radiation is measured to be 820 W/m² at noon. The maximum ambient temperature is found to be 42 °C at 14:00 h of the typical day.

According to the measured data in this study, the collector exit temperature is relatively lower throughout the day for a collector height of 400 mm compared to a 170 mm collector height. So, it can be concluded that whenever the height of the collector from the ground is higher, the collector exit temperature will be lower at indicated fixed geometrical configurations, since the hotter air beneath the collector is taken away by local wind speed recorded during the experiment ranging above 6.8 m/s which is 22.2% above the yearly average wind speed of 5.3 m/s in Addis Ababa and the air with higher density flows over the collector instead of going beneath the collector.

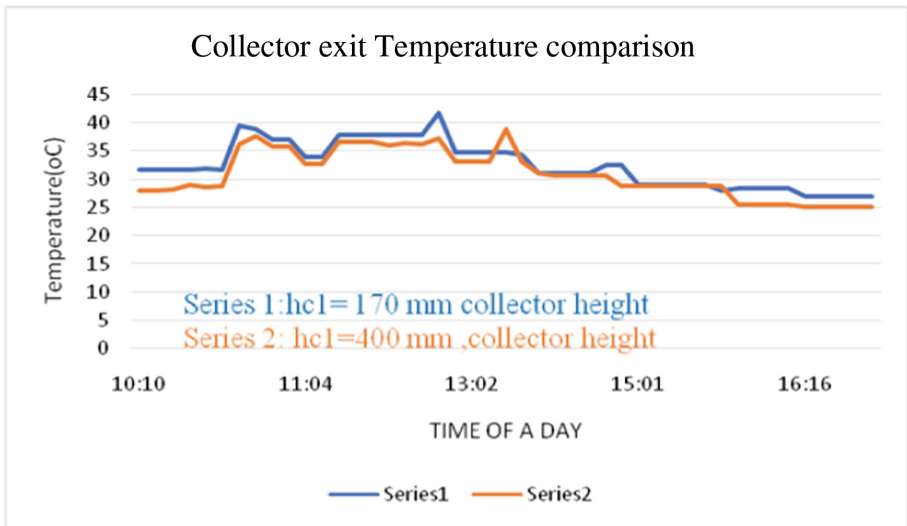


Fig. 16. Collector exit temperature comparison for different collector heights from the ground

I. Power Output vs Time of the Day

The validation for both simulated models and experimental result power output depends on the temperature difference throughout the day. So, the power output of the actual experiment varies from 8 W–32 W, maximum power output was recorded during the mid-day at 12 : 44 PM and minimum at 15 : 19 PM. While, the simulated model power output varies from 20 W–34 W, maximum at 13 : 20 PM and minimum at 10 : 10 AM as shown in Fig. 17.

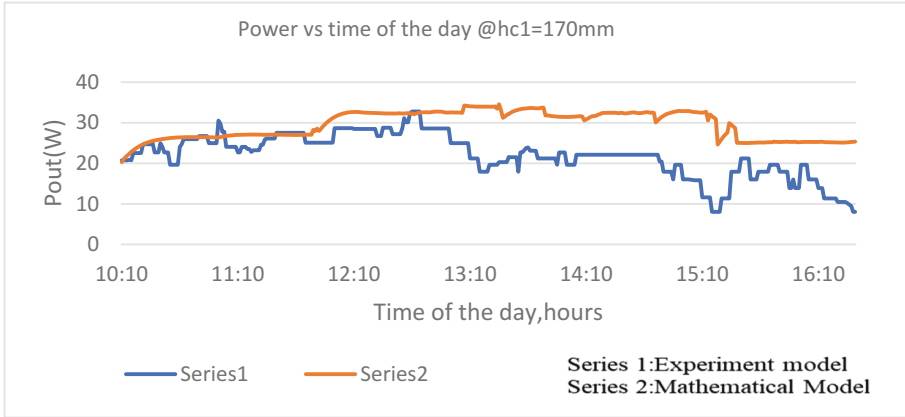


Fig. 17. Power output for an actual experiment vs mathematical model

The recorded variation is slightly different for the experimental model and CFD analysis since during the testing process the weather condition is not steady as anticipated in the historical data. In Ethiopia, the weather condition is not stable since the draught occurred in 2015 (USAID 2016). In the actual experiment, the characteristics of power output are rough as a result of collector exit temperature variation throughout the day. While in the CFD model, show that the power output throughout the day is uniform for a specified time of the day. So experimental validation is mandatory for this system before proceeding to the construction of medium to large scale solar chimney power plant, subsequently drawing a result from a CFD analysis will lead to over prediction of power output from a solar chimney power plant.

4 Conclusions

In this study, the experimental model and CFD model of the solar chimney power plant are developed for the investigation of power generation. Comparison between experimental result and CFD model shows a slight variation in maximum power output. In the CFD model total power output of 34 W is recorded for collector diameter ($D_{coll} = 2$ m), chimney diameter ($D_{chim} = 0.16$ m), and collector height from 0.17 m

up to 0.4 m above the ground, whereas in the experiment 32 W power output is recorded for same geometrical size. However in the daily power out the experimental model has an unsteady result relative to the CFD model. Additionally, optimization of the solar chimney power plant is investigated. Under a fixed chimney height from the ground ($h_{c1} = 0.170$ m), collector diameter ($D_{coll} = 2$ m), and chimney diameter ($D_{chim} = 0.16$ m), the optimum chimney height is 52 m, an increase in chimney height beyond 52 m will result in power loss due to frictional pressure drop in a chimney. Therefore, optimum chimney height for a desired potential has to be determined before the actual power plant’s development. Moreover, the study investigates the power output for a larger size. For the design of 30 kW power output, the chimney height of 15 m and collector diameter of 15 m at a fixed chimney diameter of 0.2 m and 0.2m height of the collector from the ground is the optimum size. However, making any modification to the fixed parameters results in a new optimum chimney height and collector diameter. Increasing the collector diameter increases collector exit temperature resulting in an increased power output of the plant since the longer air takes to reach the collector exit the more it gains heat. So an increase in collector diameter will increase power output. The temperature measured from the experimental study and analytical model has similarities and variations throughout the day. It should be noted that the result from the analytical model may lead to over-prediction of power output from the plant, so it is important to test the potential of the system by developing an actual experimental model before developing a large-scale solar chimney power plant.

Nomenclature

Abbreviation and symbol	Abbreviation and symbol	Greek symbols
abs : absorber	Q : Heat gain [W/m^2]	α : absorption coefficient
E_{eff} : Effectiveness of coefficient	T_a : Temperature of the air inside the collector [K]	B: coefficient of volumetric thermal expansion, 1/K
gz :glazing	T_{pm} : Mean plate temperature [K]	Δp :pressure drop, Pa
h_{c1} : Glazing height from ground at entrance[m]	T_p : Average temperature of a plate [K]	g : specific heat ratio
h_{c2} : Glazing height from ground at exit[m]	T_1 : Temperature at collector inlet	η : Efficiency
H : Chimney height[m]	T_2 : Temperature at collector exit	μ : dynamic coefficient
Δp_{tot} : Total pressure difference	T_3 : Temperature at chimney inlet	f :friction factor
P_1 : Pressure at collector inlet	T_4 : Temperature at chimney exit	ν : viscosity
P_2 : pressure at collector exit	SCPP : solar chimney power plant	τ : transmittance
P_3 : pressure at chimney inlet	V : Flow velocity [m/s]	γ :isentropic constant
P_4 : pressure at chimney exit	Agz=area of the glazing	$\rho =$ Air density, kg/m3
Rc,c-a: heat transfer from collector to ambient by convection	Vr :radial velocity of air(m/s)	
Rr,g-c: heat transfer from ground to collector by radiation	q'' :Heat flux in W/m^2	
Rc,c-f: Heat transfer from collector to the fluid(air) by convection	Rc,g-f: heat transfer from ground to fluid by convention	

Acknowledgments. The authors of this manuscript are thankful to Addis Ababa institute of technology laboratory directorate for their cooperation in providing necessary tools during experiment development.

Author Contributions. Ashenafi Tesfaye is the main author of this manuscript under the guidance of Solomon T/Mariam and Tewodros walle. All authors read and approved the final manuscript.

Funding. It is to declare that no funding for research has been received during data collection, design, and experimentation from any funding agency.

Availability of Data and Material. The data sets supporting the conclusion of this article are included within the article.

Competing Interest. The authors declare that they have no competing interests.

References

- Asnaghi, A., Ladjevardi, S.M.: Solar chimney power plant performance in Iran. *Renew. Sustain. Energy Rev.* **16**(5), 3383–3390 (2012). <https://doi.org/10.1016/j.rser.2012.02.017>
- Backström, T.W.V., Gannon, A.J., Backstro, T.W.V.: Solar chimney cycle analysis with system loss and solar collector performance with system loss and solar (2000). <https://doi.org/10.1115/1.1314379>
- Dehghani, S., Mohammadi, A.H.: Optimum dimension of geometric parameters of solar chimney power plants - A multi-objective optimization approach. *Sol. Energy* **105**, 603–612 (2014). <https://doi.org/10.1016/j.solener.2014.04.006>
- Fallah, S.H., Valipour, M.S.: Evaluation of solar chimney power plant performance: the effect of artificial roughness of collector. *Sol. Energy* **188**(May), 175–184 (2019). <https://doi.org/10.1016/j.solener.2019.05.065>
- Gannon, A.J., Backström, T.V.: Solar chimney turbine performance. *J. Sol. Energy Eng.-Trans. Asme* **125**, 101–106 (2003)
- Hamdan, M.O.: Analysis of a solar chimney power plant in the Arabian Gulf region. *Renew. Energy*, 1–6 (2010). <https://doi.org/10.1016/j.renene.2010.05.002>
- Koonsrisuk, A., Lorente, S., Bejan, A.: Constructal solar chimney configuration. *Int. J. Heat Mass Transf.* **53**(1–3), 327–333 (2010). <https://doi.org/10.1016/j.ijheatmasstransfer.2009.09.026>
- Koonsrisuk, A., Chitsomboon, T.: Mathematical modeling of solar chimney power plants. *Energy* **51**, 314–322 (2013). <https://doi.org/10.1016/j.energy.2012.10.038>
- Lal, S., Kaushik, S.C., Hans, R.: Experimental investigation and CFD simulation studies of a laboratory scale solar chimney for power generation. *Sustain. Energy Technol. Assess.* **13**, 13–22 (2016). <https://doi.org/10.1016/j.seta.2015.11.005>
- Ming, T.Z., et al.: Simple analysis on thermal performance of solar chimney power generation systems. 9671(December) (2016) <https://doi.org/10.1179/014426009X12519696923902>
- Renewable, I., Agency, E.: Renewable Energy Statistics 2017 Statistiques D ' Énergie Renouvelable 2017 Estadísticas De Energía (2017)
- Renewable, U., Program, E., Final, D.: Federal Democratic Republic of Ethiopia Ministry of Water and Energy. January (2012)
- USAID: El niño in ethiopia, a real-time review of impacts and responses 2015–2016, 28 March 2016. <http://www.agri-learning-ethiopia.org/wp-content/uploads/2016/06/AKLDP-El-Nino-Review-March-2016.pdf>
- von Backström, T.W., Gannon, A.J.: Solar chimney turbine characteristics. *Sol. Energy* **76**(1–3), 235–241 (2004). <https://doi.org/10.1016/j.solener.2003.08.009>
- Zhou, X., Xiao, B., Liu, W., Guo, X., Yang, J., Fan, J.: Comparison of classical solar chimney power system and combined solar chimney system for power generation and seaw (2010)